JACS
JOURNAL OF THE AMERICAN CHEMICAL SOCIETY
Article
pubs.acs.org/JACS

Ultrafast Dynamics of a Spiropyran in Water

Jörg Kohl-Landgraf,[†] Markus Braun,[†] Cem Özçoban,[‡] Diana P. N. Gonçalves,[‡] Alexander Heckel,[‡] and Josef Wachtveitl*,[†]

[†]Institute for Physical und Theoretical Chemistry, Goethe University Frankfurt, Max-von-Laue-Straße 7, Frankfurt/Main, Germany
[‡]Institute for Organic Chemistry and Chemical Biology, Buchmann Institute for Molecular Life Sciences, Cluster of Excellence Macromolecular Complexes, Goethe University Frankfurt, Max-von-Laue-Straße 9, Frankfurt/Main, Germany

Supporting Information

ABSTRACT: The reversible switching of a water-soluble spiropyran compound is recorded over 1 ns by means of femtosecond vis-pump/vis- and IR-probe spectroscopy under aqueous conditions. Our investigations reveal that the photochemical conversion from the closed spiropyran to the open merocyanine takes 1.6 ps whereas the reversed photoreaction is accomplished within 25 ps. The combination of time-resolved and steady-state observations allows us to reveal central parts of the reaction pathway leading to either form. The enhanced water solubility, its fast and efficient switching behavior, and its stability against hydrolysis over a time range of several weeks make this compound an attractive and versatile tool for biological applications.

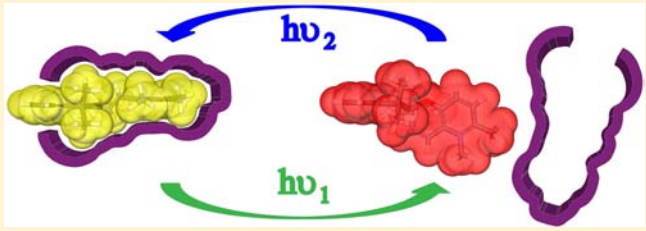

INTRODUCTION

Photochromism is the ability of a molecule to undergo reversible structural changes upon absorption of a photon.[1] Very interesting experiments become possible if the photochromic effect is coupled to a change in material properties or a biological process. Since light is an ideal—and, if applied correctly, harmless and selective—external trigger signal, this approach can confer a sophisticated level of spatiotemporal and dose control to an experiment. A recent review on "optochemical genetics" summarizes fascinating studies.[2] Also reversibly light-switchable DNA nanoarchitectures have recently come within reach.[3,4]

Putting an effect under the control of a reversible photoswitch is by far not easy. The photoswitch must be installed in such a way that the effects of its photoisomerization dominate the activities of the system to be switched as much as possible, and for biological applications the photoswitch needs to operate in an aqueous environment. Even then, the efficiency and speed of these switching processes strongly depend on the nature of the substituents and solvent conditions like (local) polarity and viscosity.[5] Hence also the performance of the photoswitch itself is a limiting factor for the switching amplitude. This motivates the ongoing search for the ideal photoswitch. Photoswitches can work for example via changes in polarity, conductivity, or hinge properties. The higher the change in these properties upon photoswitching and the better the ratio of the two isomers can be switched, the bigger the effect.

Well-known photochromic organic molecules are azobenzenes, fulgides, and spiropyrans.[6−8] While many applications are based on the cis−trans isomerization of azobenzenes, spiropyrans offer promising alternatives as photoswitches since they can be accumulated to a high degree in one state. They consist of two almost non-interacting orthogonal moieties, the chromene and the indoline (Scheme 1). The dynamics of various derivatives of these compounds has been studied in the visible and infrared spectral range on all time scales ranging from the second to the femtosecond regime, revealing that excitation in the UV range converts the molecule into the open and colored merocyanine form, which is converted back either thermally to the spiropyran form or after absorbing another photon of a different wavelength.[9−14] The mechanism of photocoloration is started by the cleavage of the C−O bond connecting the chromene with the indoline moiety. The cleaved molecule either re-establishes the bond or undergoes an isomerization process toward a stable merocyanine isomer,

Scheme 1. Spiropyran (Left) and Merocyanine Photoisomers (Right) of BIPS (a) and the Py-BIPS Compound (b)

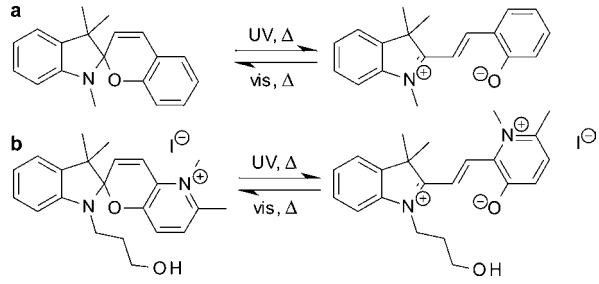

Received: May 7, 2012
Published: July 17, 2012

© 2012 American Chemical Society

dx.doi.org/10.1021/ja304395k | J. Am. Chem. Soc. 2012, 134, 14070−14077

Scheme 2. Synthesis of the Py-BIPS Compound

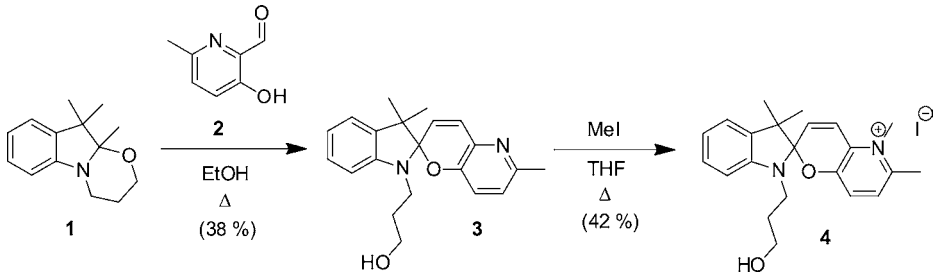

which is characterized by a strong absorbance in the visible spectral range. The shift of the absorbance from the UV into the visible spectral range is explained by the planarity of the merocyanine molecule that allows the previously uncoupled π-systems of chromene and indoline to become extended across the entire structure.[15,16] In principle the merocyanine can exist in eight different isomers depending on the orientation of the three central C−C bonds, but only isomers with a trans configuration (MC-trans) around the central bond and a cis−cis−trans isomer (MC-CCT) have been found to be stable.[16−18] The large change in dipole moment, the strong change in geometry (from perpendicular to flat), and the excellent switching ratios make photochromic spiropyrans versatile tools for a wide variety of applications such as data storage, temperature measurement, and as a trigger for biological reactions.[18−26]

The most studied spiropyran is a nitro-substituted 1′,3′,3′-trimethylspiro[2*H*-1-benzopyran-2,2-indoline] called nitro-BIPS having the nitro group in the 6 position of the chromene moiety. It has been subjected to various biological environments like RNA,[24] DNA,[22] and proteins[27] with the drawback of a (sometimes total) loss of switching efficiency in the presence of a biomolecule.[28] In addition, nitro-BIPS has been found to undergo hydrolysis under aqueous conditions.[29,30] In contrast to the nitro derivatives, the unsubstituted BIPS (compound **a** in Scheme 1) does not involve triplet states along the reaction pathway,[17] and the thermal equilibrium is shifted toward the closed spiropyran because the electron-withdrawing nitro substituent is missing and the bond between the spiro carbon atom and the oxygen is stronger. However, it is barely soluble in water. In contrast, a two-fold nitro-substituted compound (dinitro-BIPS) seems to involve only singlet states along the reaction pathway.[14,31−33]

In general, the closed spiropyran form has no absorbance in the visible spectral range but pronounced absorbance peaks in the middle and near UV, whereas the merocyanine form is dominated by a strong absorption in the visible range whose position shifts with solvent polarity, indicating a zwitterionic structure.[34] The time constant for the opening and subsequent isomerization reaction of BIPS in ethanol and tetrachloroethene was found to be 1.3 ps by probing the dynamics in the visible[16] and 28 ps in the mid-IR.[35] The main deactivation from the S1 state happens via a conical intersection to the spiropyran ground state with a probability of 90%. The remaining 10% is forming an intermediate state.[13,36,37] The conical intersection results from an intersection of the ground and first excited singlet energy surfaces and corresponds to a configuration at which the spiro-carbon bond to the oxygen is cleaved but no isomerization has taken place yet.[38] The intermediate state has been identified to be a conformation called cis−cis−cis merocyanine (MC-CCC) from which the merocyanine isomerizes toward a stable MC-trans isomer.[10,36,39−43] To our knowledge no time-resolved experimental data on the closing reaction of unsubstituted BIPS are available yet, even though there exist a few theoretical studies dealing with it.[44,45]

Although the photoreaction of these molecules is well studied in various solvents, there is only very limited information available on the ground-state behavior not to mention the excited-state dynamics in aqueous solution, which is of crucial importance especially for a potential biological application. To fulfill our needs for an efficient, water-soluble, and also stable compound, we chose to study a spiropyran with an enhanced water solubility, due to a pyridinium structure in the right part of the molecule (compound **b** in Scheme 1). We will refer to it as Py-BIPS in the following. It is a derivative of the BIPS molecule and does not contain a nitro group. Py-BIPS was originally introduced by Yu et al. and has been used so far primarily for (solid-state) material applications, including for example switching of magnetic properties or in molecular logics.[46−48] To reveal the efficiency and speed limit of the opening and also the closing process under aqueous conditions we combine steady-state observations and femtosecond transient absorption measurements in the visible and infrared spectral range. Besides following the excited-state dynamics in the femtosecond and picosecond regime under such solvent conditions, this is also the first experimental investigation on the closing reaction of a spiropyran in that time regime that is not nitro-substituted.

EXPERIMENTAL SECTION

Steady State. UV/vis steady-state spectra were taken on a Specord S100 from Analytic Jena. The merocyanine absorbance at 350 nm was determined in an HPLC analysis which was used to estimate the change in spiropyran concentration upon UV irradiation. From that the merocyanine concentration after UV irradiation could be evaluated, and in combination with an absorption spectrum the extinction coefficient could be determined.

Transient Absorption in the UV/Vis. The source for the femtosecond laser pulses was a Clark CPA 2001 laser system providing 170 fs pulses at 1 kHz repetition rate and an average output power of 800 mW centered around 775 nm.

For the generation of the 520 nm pump pulses a non-collinear optical parametric amplifier (NOPA) process was used with subsequent compression of the pulses in a prism compressor. The pump pulses in the UV range at 350 nm were produced by sum frequency generation (SFG) of 640 nm NOPA output and 775 nm fundamental pulses in a BBO crystal. The broadband probe pulses were created by focusing a small fraction of the fundamental pulses into a 5 mm thick CaF_2 crystal which was moved during the measurement to avoid material degradation, thus creating a super-continuum white light. The measured transient spectra were corrected for coherent effects around delay time zero and for the chirp of the probe light. The angle between pump and probe polarization was set to the magic angle at 54.7° to eliminate anisotropic contributions. The

dx.doi.org/10.1021/ja304395k | J. Am. Chem. Soc. 2012, 134, 14070−14077

sample was diluted in analytical grade water (Acros Organics) to a concentration of 1 mM and placed in a 1 mm quartz cuvette. The temporal resolution was found to be around 220 fs for the experiment with UV excitation and 100 fs for the 520 nm excitation.

Transient Absorption in the Mid-IR. The probe pulses in the mid-IR were created as described by Hamm et al.[49] in a two-step OPA process with subsequent difference frequency mixing. The pump pulses were generated as described above but without subsequent pulse compression, resulting in a temporal resolution of 500 fs. The sample was diluted in D_2O (Euriso-Top, 99.96%) to a concentration of 20 mM and placed between two CaF_2 plates which were separated by a 50 μm thick spacer.

Experimental Conditions. During the measurements the sample was, with the aid of color filters, irradiated with monochromatic light from a HgXe arc lamp to accumulate the desired isomeric state: for merocyanine accumulation UG1 and WG320 filters from Schott AG were used, and for the spiropyran accumulation a GG420 color glass filter was used. Quantitative analysis was performed by fitting the data with a set of exponential decay functions with wavelength-dependent amplitudes as described elsewhere.[50]

Synthesis. All reactions were performed under an argon atmosphere using dry solvents. NMR spectra were recorded on Bruker AM 250 and AV 400 MHz instruments. To assign proton shifts additional $^1H-^1H$ COSY experiments were performed. An overview of the synthesis can be found in Scheme 2. Compound **1** was synthesized in analogy to the method reported by Beyer et al.[51] Compound **2** was synthesized in analogy to the method reported by Daines et al.,[52] where 210 mg (1.53 mmol) of 3-hydroxy-6-methyl-2-pyridinecarboxyaldehyde **2** was dissolved in 10 mL of dry EtOH. To the pale yellow solution was added 300 mg (1.38 mmol) of indoline **1** dropwise, and the dark-violet mixture was refluxed for 5 h. The ethanol was almost evaporated, and 10 mL of cold water was added. The mixture was stirred in an ice bath overnight. The resulting precipitate was filtered, washed with water, and dried under vacuum to yield 174 mg (0.517 mmol) of compound **3** (38%) as brown crystals. ^1H NMR (400 MHz, $CDCl_3$): δ = 7.2–7.15 (m, 1H, H_{ar}), 7.07 (d, J = 7.1 Hz, 1H, H_{ar}), 7.02 (d, J = 10.5 Hz, 1H, H_{ar}), 6.9–6.83 (m, 3H, H_{ar}), 6.62 (d, J = 8.1 Hz, 1H, H_{ar}), 5.95 (d, J = 10.2 Hz, 1H, H_{ar}), 3.71 (t, J = 5.6 Hz, 2H, $-CH_2$), 3.43–3.21 (m, 2H, $-CH_2$), 2.45 (s, 3H, Ar$-CH_3$), 1.98–1.78 (m, 2H, $-CH_2$), 1.25 (s, 3H, $-CH_3$), 1.13 (s, 3H, $-CH_3$) ppm. ^{13}C NMR (100.6 MHz, $CDCl_3$): δ = 149.7, 149.1, 147.5, 137.7, 136.5, 131.3, 127.8, 124.2, 124.0, 122.6, 121.8, 119.4, 106.8, 105.2, 61.0, 52.5, 41.0, 31.9, 25.9, 23.5, 20.3 ppm. MALDI-HRMS: m/z calcd for $C_{21}H_{24}N_2O_2$ $[M+H]^+$ 337.19105, found 337.19134 (Δm 0.00029, error 0.86 ppm).

Next, 0.13 g (0.39 mmol) of the neutral spiropyran **3** was dissolved in 10 mL of dry THF. To the brown solution was added 0.1 mL (1.61 mmol) of iodomethane, and the mixture was refluxed overnight. The solution was cooled to room temperature, and the resulting yellow microcrystalline solid was filtered, washed with THF, and dried to yield 70 mg (0.15 mmol) of spiro[2*H*-indole-2,2′-[2*H*]pyrano[3,2-b]pyridinium]-1-(2-hydroxypropyl)-3,3,5′,6′-tetramethyl iodide (Py-BIPS, derivative **4**, 42%) as a yellow solid. ^1H NMR (250 MHz, DMSO): δ = 7.87 (d, J = 8.7 Hz, 1H, H_{ar}), 7.73 (d, J = 3.9 Hz, 1H, H_{ar}), 7.69 (d, J = 6.1 Hz, 1H, H_{ar}), 7.17–7.11 (m, 2H, H_{ar}), 6.81 (dd, J = 7.3, 14.7 Hz, 1H, H_{ar}), 6.68 (d, J = 8.0 Hz, 1H, H_{ar}), 6.61 (d, J = 11.1 Hz, 1H, H_{ar}), 4.15 (s, 3H, $R_2N^+-CH_3$), 3.43 (t, J = 6.0 Hz, 2H, $-CH_2$), 3.38–3.13 (m, 2H, $-CH_2$), 2.70 (s, 3H, Ar$-CH_3$), 1.85–1.56 (m, 2H, $-CH_2$), 1.25 (s, 3H, $-CH_3$), 1.13 (s, 3H, $-CH_3$) ppm. ^{13}C NMR (62.9 MHz, DMSO): δ = 150.8, 147.7, 146.4, 135.0, 134.0, 131.5, 130.3, 128.6, 127.8, 122.0, 121.7, 119.3, 106.6, 106.0, 58.2, 53.2, 31.4, 25.4, 20.5, 19.7 ppm. MALDI-HRMS: m/z calcd for $C_{22}H_{27}N_2O_2^+$ $[M]^+$ 351.2067, found 351.20746 (Δm 0.00076, error 2.16 ppm)

RESULTS AND DISCUSSION

Steady-State Observations. At thermal equilibrium the Py-BIPS compound is mainly in the closed spiropyran form. Notably, Py-BIPS showed an excellent solubility in PBS buffer (see Supporting Information). The content of merocyanine is about 2.5%. The degradation time due to hydrolysis was estimated by a series of absorption measurements of a sealed cuvette performed over 25 weeks. The spectral analysis of the disappearance of the spiropyran absorption peak at 350 nm yields a half-life time for degradation of 1350 h (data not shown). By illumination with visible light the closed spiropyran can be accumulated to nearly 100%, resulting in a slightly yellowish solution that exhibits a strong absorbance in the near UV around 350 nm (gray curve in Figure 1). This peak is

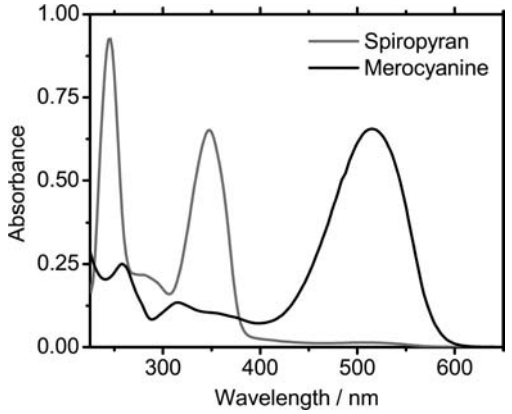

Figure 1. Absorption spectra in water during HPLC analysis of a sample of Py-BIPS after 2 min of UV irradiation. Py-BIPS, gray curve; merocyanine form, black curve. The presence of merocyanine is evidenced by a pronounced peak in the visible range centered around 520 nm.

ascribed to the S0→S1 transition of the spiropyran. In contrast to the S0→S1 transition of unsubstituted BIPS, which mainly results from the pyrano[3,2-b]pyridinium moiety, this absorption maximum of Py-BIPS is shifted about 50 nm toward longer wavelengths, which is valuable for biological applications. This effect has also been observed in THF and in crystalline structure.[48,53]

After accumulation of merocyanine by illumination with monochromatic UV light, the absorption spectrum is dominated by a band around 520 nm that can be ascribed to the S0→S1 transition of the open form (black curve Figure 1).[37] The quantum yield of the opening reaction was estimated by irradiating the sample over a certain time interval with a defined intensity at 350 nm and measuring the absorbance change at the position of the product absorption at 520 nm, where an extinction coefficient of the merocyanine of 19 400 l/mol·cm was found. The quantum yield was found to be 3.3% for the opening reaction, which is in agreement with values found for unsubstituted BIPS of <10%.[35] Efficiencies for nitro-BIPS range from 11% in acetonitrile up to 83% in methylcyclohexane,[42] whereas for dinitro-BIPS in chloroform 9% was found.[14] To our knowledge there is no value for the quantum efficiency of the closing reaction of the BIPS compound available in literature yet. We estimated that efficiency by the recovery ratio of bleached ground state modes of the transient vis pump-IR probe experiments discussed below to be ≤20%. For nitro-BIPS a 10% efficiency in toluol and for dinitro-BIPS 40% in chloroform were estimated.[14,54]

With continuous UV irradiation we could accumulate up to 26% merocyanine in the solution, whereas, as mentioned above,

irradiation with visible light reduces the content of merocyanine below the detection threshold. In a cyclic switching experiment (shown in the Supporting Information) where the whole solution was irradiated with alternating UV and visible light, we found that a single molecule could be switched back and forth more than seven times before decomposition.

The Opening Reaction. The transient absorption spectrum of the closed spiropyran of the Py-BIPS compound after photoexcitation at 350 nm (Figure 2) is dominated by two

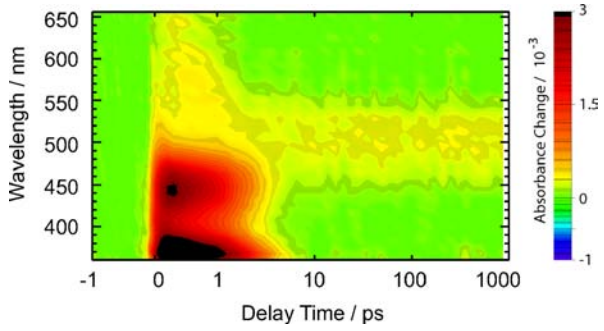

Figure 2. Transient absorption spectrum of the Py-BIPS compound in water for the conversion from spiropyran to merocyanine in the visible spectral range after 350 nm excitation. The absorbance change caused by product formation is weakly visible around 520 nm. The time scale in this and the following transient spectra is linear below 1 ps and logarithmic above.

positive absorption changes centered at 380 and 450 nm that appear within the temporal resolution. They are a result of excited-state absorption from the spiropyran S1 state to higher states.[16] In addition a weak unstructured feature appears from 500 to 650 nm. The absorbance change caused by the merocyanine product is apparent after about 1 ps by a weak positive absorption feature which preserves its spectral shape on longer time scales. Kinetic analysis was performed from 0.5 ps onward where the signal is completely free of coherent effects that occur around delay time zero and are mainly a result of cross-phase modulation of pump and probe pulse in the solvent.[55] Two time constants were required to describe the dynamics adequately. A time constant of 1.6 ps models the decay of the excited state, which is in agreement with a 1.3 ps time constant found in earlier measurements on BIPS by probing the dynamics in the visible spectral range.[16] An infinite time constant describes the residual absorbance change at long delay times caused by the merocyanine product (Figure 3). Comparing the decay associated spectra of the infinite time constant with the steady-state spectrum of the merocyanine absorbance at 520 nm shows only a slight red shift of the steady-state spectrum with respect to the decay-associated spectrum for the infinite time constant, indicating that a further isomerization after forming merocyanine or a change in the merocyanine isomer ratio takes place on a longer time scale. Nevertheless the formation of open merocyanine is accomplished after the relaxation of the excited state. The common interpretation of the photocoloration process is a pathway through a conical intersection of the excited- and ground-state potential energy surfaces from which either the spiropyran ground state is repopulated or the merocyanine product is formed.[38] In our case the pathway leading to the repopulation of the spiropyran ground state is very efficient since the fraction of merocyanine formed is only 3.3%. The interpretation of the

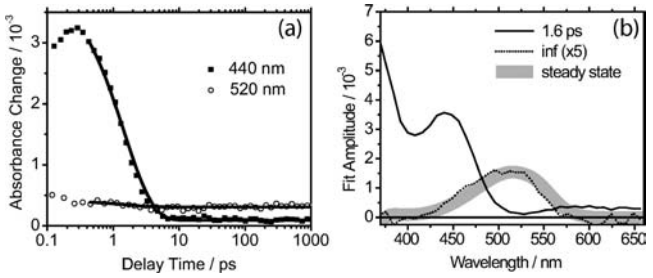

Figure 3. Kinetic analysis of the opening reaction. (a) Single transients at wavelengths indicative for excited-state absorption at 440 nm and for product formation at 520 nm. (b) Decay-associated spectra (DAS) of the two time constants found in the fitting procedure and a scaled steady-state difference spectrum. The DAS of the infinite time constant was scaled by a factor of 5 for a better representation.

broad absorbance above 550 nm is difficult since it is rather featureless across the observed spectral range. The formation of a triplet state can be excluded, because the decay and especially the rise time of the signal are too fast. Values for the lifetime of a triplet state in BIPS were found to be in the μs range.[36] From the time-resolved observations we can conclude that the formation of merocyanine in its ground state happens directly and without the involvement of stable intermediate states or isomers in the excited state since we find only a monoexponential decay of the excited-state absorption.

The Closing Reaction. The transient absorption spectrum of the merocyanine form of the Py-BIPS compound in the visible spectral range after photoexcitation at 520 nm (Figure 4)

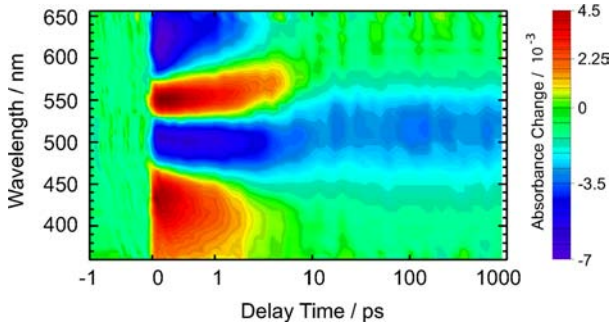

Figure 4. Transient absorption spectrum of the Py-BIPS compound in water for the conversion from merocyanine to spiropyran in the visible spectral range after 520 nm excitation. The remanent bleaching of the merocyanine absorbance due to ring closure is apparent around 520 nm.

is dominated by a signal of the bleached ground state around 520 nm, which is more intense at early delay times and subsequently recovers until it preserves its spectral shape throughout the measurement range from about 10 ps onward. In addition two positive absorption features can be observed at 350−460 and 540−580 nm. At 580−660 nm another negative absorption feature is apparent. To describe the dynamics observed in the visible range properly, three time constants are required. The decay associated spectra shown in Figure 5 do overlap, indicating that the temporal development of the spectral features cannot be described with a single exponential function. What can be seen at the amplitudes is that the positive absorption features both involve a 3.2 ps time constant, allowing the interpretation that they are only a single feature that is spectrally superimposed with the contribution of the

dx.doi.org/10.1021/ja304395k | J. Am. Chem. Soc. 2012, 134, 14070−14077

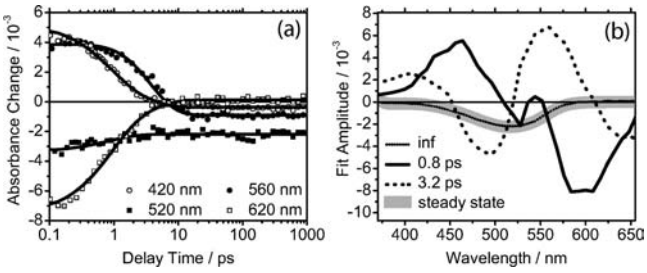

Figure 5. Kinetic analysis of the closing reaction of the Py-BIPS compound in water in the visible spectral range. (a) Single transients selected in regions with dominant contribution from excited-state absorption (420 and 560 nm), stimulated emission (620 nm), and bleached ground state (520 nm). (b) Decay-associated spectra of the three time constants found in the fitting procedure and a scaled steady-state difference spectrum.

ground-state bleach at 520 nm. This time constant also appears in the decay signal of the stimulated emission and the recovery of the ground-state bleach. On the other hand the 0.8 ps time constant has maximum contributions at 470 nm (positive) and 600 nm (negative). Looking at the single transients at these wavelengths shows that this time constant appears at spectral positions where positive absorption features are changing to negative ones toward longer delay times and vice versa. That leads to the conclusion that the 0.8 ps time constant describes spectral shifts whereas the 3.2 ps time constant is directly correlated to transitions in the electronic structure of the merocyanine compound. Excitation at 520 nm leads to a population of the S1* state that subsequently relaxes to the S1 state with a 0.8 ps time constant, resulting in a spectral shift of the excited-state absorption. The decay of the S1 state back to the merocyanine ground state is described by the 3.2 ps time constant. Therefore, the positive absorption feature can be assigned to excited-state absorption from the merocyanine S1 state and the negative feature above 590 nm to stimulated emission from that state.

Since product formation could not be observed from these measurements directly, also a vis-pump/IR-probe experiment in the range from 1290 to 1610 cm^{-1} was performed where the product bands of the closed form can be accessed (Figure 6). Other spectral ranges in the IR did not contain additional information. The transient absorption spectrum shows traces of perturbed free induction decay at 1590, 1530, 1480, and weakly at 1405 cm^{-1} indicating that the negative signals occurring at these frequencies at positive delay times result from vibrational modes of the merocyanine ground state (Figure 7b). Around delay time zero the signal is dominated by cross-phase modulation of the pump and probe pulse leading to an artifact that does not contain any information on the reaction. Therefore the kinetic analysis was performed from 1 ps onward, where the signal is completely free of coherent effects. The positive absorption changes at early delay times around 1570, 1515, 1450, and 1390 cm^{-1} result from hot vibrational merocyanine modes due to heating of the molecule upon excitation. At longer delay times product formation can be observed at 1500, 1320, and weakly at 1560 cm^{-1}. The spectral features at long delay times are in good agreement with the steady-state difference spectrum of the merocyanine → spiropyran conversion shown on the right in Figure 6, where (+) denotes positive and (−) negative absorbance changes. It was found that the data set is modeled best with a set of four time constants. Time constants of 2 and 4.5 ps describe the fast

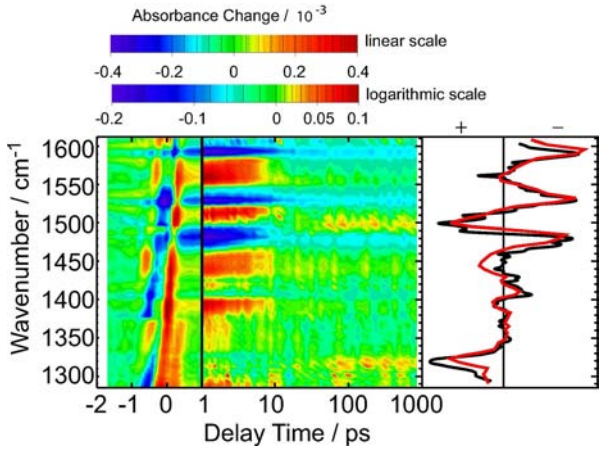

Figure 6. Left: IR transient absorption spectra of the closing reaction of the Py-BIPS compound in D_2O in the range from 1610 to 1290 cm^{-1}. For optimal representation the signal from −2 to 1 ps and the transient spectrum from 1 ps to 1 ns were drawn with independent color codes (signals above 1 ps appear 5 times stronger). Product formation is apparent at 1500 and 1320 cm^{-1}. Right: steady-state FTIR difference spectrum in D_2O of the closing reaction (black curve) and scaled decay associated spectrum of the infinite time constant. (+) and (−) indicate positive and negative absorption changes, respectively.

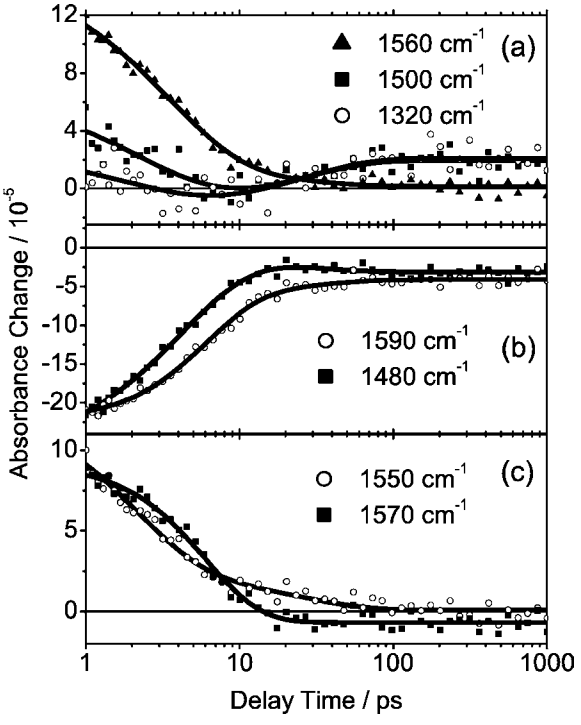

Figure 7. Kinetic analysis of the closing reaction in D_2O in the infrared spectral range. Selected transients were taken at different frequencies indicative for product formation at 1500 and 1320^{-1} (a), ground-state bleach and partial recovery at 1480 and 1590 cm^{-1} (b), and red-shifted vibrational modes at early delay times at 1550 and 1570 cm^{-1} with respect to the ground-state modes (c).

relaxation of hot vibrational modes and ground-state recovery and apply for all observed absorbance changes in the early transient spectrum. A 25 ps time constant describes the formation of the product bands at 1500, 1320, and 1560 cm^{-1} (Figure 7a). The decay of a signal with that time constant can be found at 1550 cm^{-1} (Figure 7c) and also at some

dx.doi.org/10.1021/ja304395k | J. Am. Chem. Soc. 2012, 134, 14070−14077

frequencies in the range from 1350 to 1480 cm^{-1}, which are too weak to be visible in the 3d transient plot due to the color code but appear in the fitting amplitudes. From these observations we conclude that the pathway leading to the closed spiropyran involves a hot merocyanine S0 state which is populated with the 3.2 ps time constant mentioned above. From here either the molecule cools to the vibrational merocyanine ground state or the closed spiropyran is formed within 25 ps. Since the recovery of the vibrational ground-state modes is accomplished mainly within 2−4.5 ps and to a small amount with 25 ps (1590 cm^{-1}), it is likely that the relaxation back to the merocyanine ground state takes place also from intermediate states along the reaction pathway leading to the closed form. To estimate the quantum efficiency for the closing reaction, the recovery ratio of the bleach signal at 1590 cm^{-1} has been estimated by

$$\Phi \leq \frac{A_{1000}}{A_1} \quad (1)$$

where A_1 denotes the absorbance at 1 ps after excitation in a region where the signal is free of coherent effects and A_{1000} the remaining absorbance change after 1000 ps. It has to be admitted that this way of determining the quantum efficiency is not ideal, because the bleached ground-state modes overlap spectrally with vibrations of the hot molecule at early times, but it can provide an upper limit for the yield of the reaction which was found to be 20%.

Reaction Pathway. From our measurements with the Py-BIPS compound we propose the reaction pathway shown in Scheme 3. The continuous lines indicate transitions involved in the opening reaction, whereas broken lines mark the transitions that occur during the closing reaction. Exciting the closed spiropyran at 350 nm (1) induces a population of the S1 state that has a lifetime of 1.6 ps. Excited-state absorptions to higher states can be found at 380 and 450 nm (2). The relaxation to the ground-state potential energy surface happens presumably via a conical intersection (CI) back to the spiropyran ground state (4) or, with a 3.3% probability, an isomerization toward a stable merocyanine isomer takes place (5). We did not find isomers along the reaction pathway that are significantly spectrally different from the final product. However, a slight shift can be observed between the decay-associated spectrum of the infinite time constant and the steady-state difference spectrum, indicating a redistribution between different isomers on a longer time scale, which is accounted for by an interceptor along the reaction pathway. The shift is most likely due to isomerization from a cisoid, which is formed on a short time scale, to a trans-merocyanine isomer on a longer time scale that is outside the measurement range.

Exciting the merocyanine compound to the Franck−Condon region at 520 nm (6) creates hot merocyanine in its S1* state with subsequent cooling within 0.8 ps (8) to the relaxed S1 state. An excited-state absorption from the S1 state to a higher state can be observed over a huge spectral range stretching from 350 to 580 nm (7). The S1 state decays within 3.2 ps, forming hot merocyanine in the ground state (9) from where either it relaxes by cooling back to the merocyanine ground state (10) or closed spiropyran is formed within 25 ps (11) (maybe via a cascade of several ground-state intermediates as indicated by an interceptor on the pathway). An overview of the spectroscopic and kinetic data can be found in Table 1.

Scheme 3. Reaction Pathway in a Simplified Potential Energy Scheme

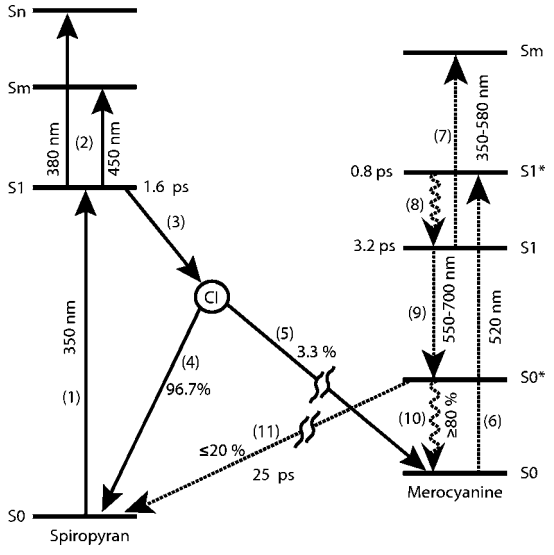

Table 1. Overview of the Spectroscopic and Kinetic Data

	SP	MC
λ_{abs} [a]	350 (300)	520 (540)
$\varepsilon_{350\ nm}$ [b]	9600 (7500)	3200
$\varepsilon_{520\ nm}$	0	19400
τ [c]	1.6 (1.3)	25
Φ [d]	0.033 (<0.1)	≤0.2

[a]Characteristic absorption (nm). [b]Extinction coefficient (l/mol·cm). [c]Formation time (ps) (SP to MC and MC to SP). [d]Quantum yield (SP to MC and MC to SP). Values in parentheses represent the values for unsubstituted BIPS.[16,35]

However, care has to be taken in comparing the efficiencies of the Py-BIPS compound with those of unsubstituted or nitro- and dinitro-substituted BIPS since they depend strongly on solvent conditions and up to now there are no values available dealing with an aqueous environment.[42] In analogy to unsubstituted BIPS and dinitro-BIPS which do not involve triplet states along the reaction pathway either, the opening reaction takes place on the excited state, and further isomerization of the different merocyanine isomers on the ground state is likely. In addition, the closing reaction takes place on the ground state since we did not find traces of excited-state absorption after the relaxation of the merocyanine S1 to a hot merocyanine S0 state. These findings are in analogy with the reaction pathway for the closing reaction proposed by Sheng et al.[40]

■ CONCLUSION

In comparison to nitro-BIPS, the Py-BIPS compound exhibits fundamental advantages that make it a versatile and powerful tool to trigger especially biological processes. One major advantage is its stability against hydrolysis which can be explained by the ratio of merocyanine in the thermal equilibrium that is, unlike nitro-BIPS, to a high degree on the spiropyran side, and merocyanine is known to degrade in an aqueous environment.[29,30] Furthermore, the solubility of Py-BIPS in water with respect to nitro- and unsubstituted BIPS appears to be much higher since we chose a pyridinium structure in the chromene part of the molecule. The lack of

dx.doi.org/10.1021/ja304395k | J. Am. Chem. Soc. 2012, 134, 14070−14077

triplet states along the reaction pathway makes Py-BIPS invulnerable to quenching mechanisms that could explain the loss of photochromism within DNA strands.[28] The switching between both Py-BIPS conformations with the respective wavelengths happens in spectral regions that turn out to be harmless to living organisms and thus opens up the avenue toward *in vivo* applications, whereas the light-triggered conformational change for nitro-BIPS is usually carried out with wavelengths below 300 nm.

It is remarkable that on the one hand the content of merocyanine can reach up to 26% whereas on the other hand a pure spiropyran solution can be prepared and that the switching is reversible for more than seven cycles, allowing for the application of established biomolecular selection strategies. The static features in combination with the fast and efficient switching behavior make Py-BIPS a valuable starting point for the synthesis of various derivatives that have to be optimized with respect to their biomolecular interaction sites. Experiments utilizing this water-soluble switch to trigger RNA activity are currently underway.

■ ASSOCIATED CONTENT

Supporting Information

HPLC conditions, absorption spectra of the photochemical and thermal equilibria, determination of the hydrolysis rate, reversible switching and fatigue resistance, comparison of solubilities of diverse spiro compounds, influence of the iodide, and fitting amplitudes for the measurement in the IR. This material is available free of charge via the Internet at http://pubs.acs.org.

■ AUTHOR INFORMATION

Corresponding Author

wveitl@theochem.uni-frankfurt.de

Notes

The authors declare no competing financial interest.

■ ACKNOWLEDGMENTS

We thank the Deutsche Forschungsgemeinschaft (DFG) for financial support through SFB 902 "Molecular Principles of RNA-based Regulation" and the Cluster of Excellence Macromolecular Complexes Frankfurt (CEF, EXC 115).

■ REFERENCES

(1) Bouas-Laurent, H.; Dürr, H. *Pure Appl. Chem.* **2001**, *73*, 639−665.
(2) Fehrentz, T.; Schönberger, M.; Trauner, D. *Angew. Chem., Int. Ed.* **2011**, *50*, 12156−12182.
(3) Tanaka, F.; Mochizuki, T.; Liang, X.; Asanuma, H.; Tanaka, S.; Suzuki, K.; Kitamura, S.-i.; Nishikawa, A.; Ui-Tei, K.; Hagiya, M. *Nano Lett.* **2010**, *10*, 3560−3565.
(4) Nishioka, H.; Liang, X.; Kato, T.; Asanuma, H. *Angew. Chem., Int. Ed.* **2012**, *51*, 1165−1168.
(5) Harriman, A. *J. Photochem. Photobiol., A* **1992**, *65*, 79−93.
(6) Yokoyama, Y. *Chem. Rev.* **2000**, *100*, 1717−1740.
(7) El Halabieh, R. H.; Mermut, O.; Barrett, C. J. *Pure Appl. Chem.* **2004**, *76*, 1445−1465.
(8) Tamai, N.; Miyasaka, H. *Chem. Rev.* **2000**, *100*, 1875−1890.
(9) Krongauz, V. A.; Golinelli, A. *Polym. Bull.* **1982**, *6*, 259−262.
(10) Chibisov, A. K.; Görner, H. *J. Phys. Chem. A* **1997**, *101*, 4305−4312.
(11) Holm, A.-K.; Rini, M.; Nibbering, E. T. J.; Fidder, H. *Chem. Phys. Lett.* **2003**, *376*, 214−219.
(12) Futami, Y.; Chin, M. L. S.; Kudoh, S.; Takayanagi, M.; Nakata, M. *Chem. Phys. Lett.* **2003**, *370*, 460−468.
(13) Holm, A.-K.; Mohammed, O. F.; Rini, M.; Mukhtar, E.; Nibbering, E. T. J.; Fidder, H. *J. Phys. Chem. A* **2005**, *109*, 8962−8968.
(14) Buback, J.; Kullmann, M.; Langhojer, F.; Nuernberger, P.; Schmidt, R.; Würthner, F.; Brixner, T. *J. Am. Chem. Soc.* **2010**, *132*, 16510−16519.
(15) Tyer, N. W.; Becker, R. S. *J. Am. Chem. Soc.* **1970**, *92*, 1289−1294.
(16) Ernsting, N. P. *Chem. Phys. Lett.* **1989**, *159*, 526−531.
(17) Ernsting, N. P.; Arthen-Engeland, T. *J. Phys. Chem.* **1991**, *95*, 5502−5509.
(18) Ernsting, N. P.; Dick, B.; Arthen-Engeland, T. *Pure Appl. Chem.* **1990**, *62*, 1483−1488.
(19) Berkovic, G.; Krongauz, V.; Weiss, V. *Chem. Rev.* **2000**, *100*, 1741−1754.
(20) Parthenopoulos, D. A.; Rentzepis, P. M. *Science* **1989**, *245*, 843−845.
(21) Kawata, S.; Kawata, Y. *Chem. Rev.* **2000**, *100*, 1777−1788.
(22) Andersson, J.; Li, S.; Lincoln, P.; Andréasson, J. *J. Am. Chem. Soc.* **2008**, *130*, 11836−11837.
(23) Mayer, G.; Heckel, A. *Angew. Chem., Int. Ed.* **2006**, *45*, 4900−4921.
(24) Young, D. D.; Deiters, A. *ChemBioChem* **2008**, *9*, 1225−1228.
(25) Shiraishi, Y.; Itoh, M.; Hirai, T. *Phys. Chem. Chem. Phys.* **2010**, *12*, 13737−13745.
(26) Poscik, A.; Wandelt, B. *Synth. Met.* **2009**, *159*, 723−728.
(27) Kocer, A.; Walko, M.; Feringa, B. L. *Nat. Protoc.* **2007**, *2*, 1426−1437.
(28) Beyer, C.; Wagenknecht, H.-A. *Synlett* **2010**, *9*, 1371−1376.
(29) Stafforst, T.; Hilvert, D. *Chem. Commun.* **2009**, 287−288.
(30) Movia, D.; Prina-Mello, A.; Volkov, Y.; Giordani, S. *Chem. Res. Toxicol.* **2010**, *23*, 1459−1466.
(31) Buback, J.; Nuernberger, P.; Kullmann, M.; Langhojer, F.; Schmidt, R.; Würthner, F.; Brixner, T. *J. Phys. Chem. A* **2011**, *115*, 3924−3935.
(32) Kullmann, M.; Ruetzel, S.; Buback, J.; Nuernberger, P.; Brixner, T. *J. Am. Chem. Soc.* **2011**, *133*, 13074−13080.
(33) Hobley, J.; Pfeifer-Fukumura, U.; Bletz, M.; Asahi, T.; Masuhara, H.; Fukumura, H. *J. Phys. Chem. A* **2002**, *106*, 2265−2270.
(34) Takahashi, H.; Yoda, K.; Isaka, H.; Ohzeki, T.; Sakaino, Y. *Chem. Phys. Lett.* **1987**, *140*, 90−94.
(35) Rini, M.; Holm, A.-K.; Nibbering, E. T. J.; Fidder, H. *J. Am. Chem. Soc.* **2003**, *125*, 3028−3034.
(36) Chibisov, A. K.; Görner, H. *Phys. Chem. Chem. Phys.* **2001**, *3*, 424−431.
(37) Fidder, H.; Rini, M.; Nibbering, E. T. J. *J. Am. Chem. Soc.* **2004**, *126*, 3789−3794.
(38) Celani, P.; Bernardi, F.; Olivucci, M.; Robb, M. A. *J. Am. Chem. Soc.* **1997**, *119*, 10815−10820.
(39) Minkin, V. I. *Chem. Rev.* **2004**, *104*, 2751−2776.
(40) Sheng, Y.; Leszczynski, J.; Garcia, A. A.; Rosario, R.; Gust, D.; Springer, J. *J. Phys. Chem. B* **2004**, *108*, 16233−16243.
(41) Chibisov, A. K.; Görner, H. *J. Phys. Chem. A* **1999**, *103*, 5211−5216.
(42) Görner, H. *Phys. Chem. Chem. Phys.* **2001**, *3*, 416−423.
(43) Zhang, J. Z.; Schwartz, B. J.; King, J. C.; Harris, C. B. *J. Am. Chem. Soc.* **1992**, *114*, 10921−10927.
(44) Gomez, I.; Reguero, M.; Robb, M. A. *J. Phys. Chem. A* **2006**, *110*, 3986−3991.
(45) Sanchez-Lozano, M.; Estévez, C. M.; Hermida-Ramón, J.; Serrano-Andres, L. *J. Phys. Chem. A* **2011**, *115*, 9128−9138.
(46) Bénard, S.; Yu, P. *Adv. Mater.* **2000**, *12*, 48−50.
(47) Bénard, S.; Rivière, E.; Yu, P.; Nakatani, K.; Delouis, J. F. *Chem. Mater.* **2001**, *13*, 159−162.
(48) Guo, X.; Zhang, D.; Zhang, G.; Zhu, D. *J. Phys. Chem. B* **2004**, *108*, 11942−1194.
(49) Hamm, P.; Kaindl, R. A.; Stenger, J. *Opt. Lett.* **2000**, *25*, 1798−1800.

(50) Neumann, K.; Verhoefen, M.-K.; Weber, I.; Glaubitz, C.; Wachtveitl, J. *Biophys. J.* **2008**, *94*, 4796−4807.
(51) Beyer, C.; Wagenknecht, H.-A. *J. Org. Chem.* **2010**, *75*, 2752−2755.
(52) Daines, R. A.; Chambers, P. A.; Pendrak, I.; Jakas, D. R.; Sarau, H. M.; Foley, J. J.; Schmidt, D. B.; Kingsbury, W. D. *J. Med. Chem.* **1993**, *36*, 3321−3332.
(53) Morgunov, R.; Mushenok, F.; Aldoshin, S.; Yur'eva, E.; Shilov, G.; Tanimoto, Y. *J. Solid State Chem.* **2009**, *182*, 1424−1429.
(54) Wohl, C. J.; Kuciauskas, D. *J. Phys. Chem. B* **2005**, *109*, 22186−22191.
(55) Dietzek, B.; Pascher, T.; Sundström, V.; Yartsev, A. *Laser Phys. Lett.* **2007**, *4*, 38−43.